



## Evaluating the Erosion and Deposition Rates and the Role of Geomorphological Indices in Mighan Watershed

Mir Asadollah Hejazi<sup>1</sup>, Ma'asumeh Rajabi<sup>1</sup>, Javad Varvani<sup>2</sup>, Atena Asgari<sup>3\*</sup>

<sup>1</sup> Associate Professor, Geomorphology Department, Tabriz University, Tabriz, Iran,

<sup>2</sup> Assistant Professor, Rangeland and Watershed Management, Islamic Azad University, Arak Branch, Iran,

<sup>3</sup> PhD undergraduate, Geomorphology Department, Tabriz University, Tabriz, Iran.

### ABSTRACT

Soil erosion is one of the most important factors annually threatening a vast part of Iran's lands and downgrades or completely destroys the quality of the agricultural lands and rangelands. In regions wherein the tectonic movements are active, the deformations resulting from soil erosion stir responses in the drainage network. The present study tries investigating the soil erosion and deposition proneness and neotectonic activities through geomorphological indices of Mighan Watershed situated in the northeastern side of Markazi Province. The study is a descriptive-analytical research that is conducted based on field investigation, library research and statistical evaluations in such a manner that various models are made to investigate the erosion and tectonic characteristics of the region. The results indicated that the lowest erosion and deposition rates in the sub-basin 6 are 104.3 t/km<sup>2</sup> and 20.5t/ km<sup>2</sup> per year and the highest erosion and deposition rates belong to sub-basin 10 with values equal to 148.7t/ km<sup>2</sup> and 27t/ km<sup>2</sup> per year, respectively. Corresponding to the results, the increase in BS morphological index causes an increase in the erosion and deposition rates but an inverse relationship was documented between geomorphological indices and AF, T, S and SL. In between, SL index was found playing a more accentuated role in the creation of erosion differences between sub-basins. In sum, the study results indicated that the deposition and erosion potentials of the studied basins in Mighan Watershed are variable and a collection of geomorphological factors are effective in this regard. It can be stated according to the results of correlation analysis between geomorphological indices and erosion and deposition values that the increase in BS (basin shape) index brings about an increase in the erosion and deposition rates. The results of multivariate regressions, as well, demonstrated that besides the inverse association between AF (asymmetry of the drainage basin) and erosion, there is a positive relationship between BS and erosion and deposition.

**Keywords:** Mighan Watershed, Soil Erosion, Sediment Production, Geomorphological Indices.

**Corresponding author:** Atena Asgari

**e-mail**✉ [asgari.atena@yahoo.com](mailto:asgari.atena@yahoo.com)

**Received:** 12 December 2017

**Accepted:** 28 March 2018

### 1. INTRODUCTION

Soil erosion is enumerated amongst the problems and issues important in environment conservation following which millions of sediment tons are annually deposited in the rivers, lakes and dams and large sums of money have to be spent for dredging their reservoirs (Goldman et al, 1968). Also, the recurrent floods as well as destruction and leaching of the roads and agricultural lands and contamination of potable water causes the humans and the ecosystem to be incurred with irreparable losses that can be mitigated and/or exacerbated by the human activities (Mohammadiha et al, 2011). To decrease the adverse effects of erosion, it is necessary to take soil conservation measures. According to the lack of sediment measurement stations in the majority of the watersheds' outlets countrywide and the inadequacy of the data, empirical models seem to be appropriate tools for generating important information layers. FAO, BLM, MPSIAC, EPM and USLE family models can be pointed out as the most widely applied empirical models amongst which factorial

scoring or FSM is one of the latest models as compared to the others. Nabipay et al (2013) dealt in a study with the consistency amount of results obtained from deposition estimation in FSM and real results. Kaviyan et al (2014) in another study parallel to the investigation of the soil erosion and deposition statuses of Sorkh Abad Watershed in Mazandaran Province firstly measured specific sediment rates visually through the investigation of dimensions of the sediments piled up behind two stone and mortar dams constructed on the watershed outlet and secondly applied EPM, PSIAC and FSM to evaluate the efficiency of them in estimating the erosion and deposition rates of the intended region. In continuation of their work, De Vente et al (2004) calibrated the abovementioned models for the same sub-basins and solved the problems that existed in the majority of the sub-basins for the calculation of deposition rates using these methods. Haregeweyn et al (2005) in a study in Ethiopia's Tigri region evaluated PSIAC and FSM models and concluded using the sediment measurements in eight dams that the deposition rates estimated by FSM are in consistency with the measured values. Haregeweyn et al (2005) tested FSM along with PSIAC model in Ethiopia and made changes in the factors and their explanations. The results showed that FSM can offer an appropriate consistency between the predicted specific

deposition rates and the estimated rates. De Vente et al (2006) in another study in Italy added landslide as the sixth factor to FSM and deduced through comparing the obtained results that the deposition rates estimated based on this method are not much compliant with the measured deposition rates acquired using the prior method wherein only five factors, namely geology, topography, vegetative cover, basin shape and gully erosion, had been taken into account. In another research, Mohammadiha et al (2011) concluded for the same basin without calibration of the main equation that the amount of deposition measured using FSM enjoys a greater deal of consistency in respect to PSIAC model. Atapour Fard et al (2012) employed FSM in a research in the north and northwestern part of Tehran Province and compared the obtained results with the deposition rates measured in nine sediment measurement stations. The identification of active tectonic regions is also of a great importance in this regard because the active tectonic in such investigations is indicative of the movements in the youngest time periods, to wit quaternary and, particularly, in Holocene and present time (Solaimani, 1999). Many of the geomorphological shapes are very much sensitive to the active tectonic movements and linearly change with them (Madadi et al, 2004). Therefore, the topographic analysis is considered as a useful instrument for measuring the shapes of the landscapes because the effect of tectonic activities on topography is very extensive (Saffari and Mansouri, 2013). Such an index as geomorphology can be employed to investigate the amount of metamorphosis resulted from tectonic activities (Ball and McFaden, 1977; Azure et al, 2002; Claire and Pinter, 2002; Silva et al, 2003; Mollin et al, 2004 and Hamduni et al, 2008). Geomorphology indices are particularly applied when studying active tectonics (Douglas et al, 2001). Also, these indices have been examined and confirmed by other researchers like Rockwell et al (1985) in southwest US and Wells et al (1988) in Costa Rican coasts. Quantitative measurement of landscapes morphology is useful in recognition of the region's characteristics, including in the tectonic activity rates' measurement (Claire and Pinter, 1996). The present study aims at investigating the erosion and deposition rates and, finally, the activeness of the neotectonic structures in Mighan Watershed through taking advantage of quantitative indices and clarifying the amount of role played by each.

**The Position of the Studied Region:**

The main watershed in Iran's Central Desert is comprised of 5 sub-basins, named Ghomrud, Gharreh Chay, Shur (Khoshkrud), Mighan Desert and Kashan Desert (Zulfaghary, 2010). Mighan's deposition basin is spread over a land reaching in area to 5528 km<sup>2</sup> some 2000 km<sup>2</sup> of which is composed of plains and 3528 km<sup>2</sup> thereof is covered with elevations overlooking the plain. The basin is consisted of Mighan seasonal lake featuring variable areas up to 106 km<sup>2</sup> and situated in an elevation range between 1660m and 1700m above sea level, Farahan and Arak alluvial plains, fans and foothills. The basin is located within the distance between Qom and Gharreh Chay basins and it has been created by less-elevated mountains situated on the southern, eastern and northern sides of the region and rolling terrains on the western part of the basin. The closest city to Mighan Watershed is Arak. There are villages within different distances to Mighan's seasonal lake around the desert. The

region is positioned in the lowest point of the watershed reaching in elevation to 1660 meters above sea level (Mirzakhani, 2011).

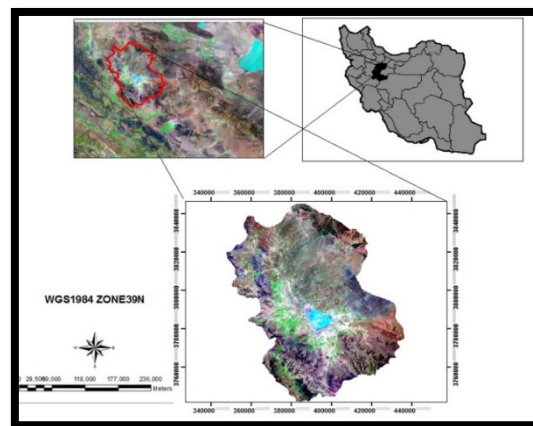


Figure 1: Mighan Watershed Position

**Geological-Structural Analysis of the Region:**

In geological structural terms, Mighan Watershed is made of two large mountainous units on the margins and one alluvial plain in its middle section. In a 1:50000 geological map of the region, Mighan Watershed is envisioned as graben system stretched along two faults. Folding and outcropping of the Paleocene era deposits on the eastern side of the watershed and the simultaneous subsidence of the middle plain as a result of the major Pasadenian tectonic movement in Paleocene era (700 thousand years ago) are the reasons that have given rise to the enclosure and independence of the watershed. The major strata and primary faults of the watershed are aligned southeast-northwestward parallel to the main tectonic axis on the flanks. The phenomenon reflects the displacements of Saudi Arabia platforms from the southwest and Cyberia from the northeast. The incident is determined after Pasadenian tectonic interval in Mighan Watershed with the onset of an erosional phase during Pleistocene. The sediments from this era include old alluvium, young alluvium, clay and salt pans accounting for a relatively vast part of the watershed (figure 2).

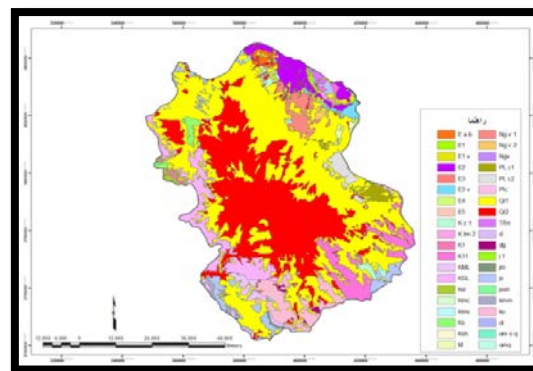


Figure 2: the scattering of geological units in Mighan Watershed (excerpt from a 1:50000 geological map)

**2. Data and Methods:**

The main instruments of the current study for the evaluation of the erosion and deposition rates and investigation of the tectonic activity status of the studied region include topographical maps (1:50000 and 1:25000), geological map (1:100000), slope, soil, vegetative cover, climatic data and satellite images of the region, repeated visits and ArcGIS 10 Software. At first, the watershed and sub-basins were delimited on the map following which the information layers were extracted. Next, various formula were applied to determine the erosion and deposition rates. In continuation, quantitative values of the geomorphological indices were obtained through quantitative analysis and correlation test of the acquired information in Mighan Watershed.

**3. Study Findings:**

**Evaluating the Erosion and Deposition Rates in the Region Using FSM:**

Ten sub-basins were extracted for the total area of Mighan Watershed. The characteristic summary of the studied ten sub-basins are given in table (1). The measured deposition rates in the sub-basins are presented in table (2).

**Table 1:** characteristics of the studied sub-basins in Mighan Watershed

Sub-basins	Average basin slope (%)	Gully status	Gravilius coefficient	Prevalent lithology
1	17.5	Very low	54.1	Alluvial terrace-limestone-shale stone, silt
2	13.8	Very low	48.1	Alluvial terrace-basalt andesite-shale-silt
3	12.7	Very low	28.1	Alluvial terrace-basalt andesite-limestone
4	14.6	Low	53.1	Alluvial terrace-basalt andesite-limestone
5	13.2	Low	67.1	Alluvial terrace-basalt andesite-limestone
6	10.4	Low	21.1	Alluvial terrace-ignimbrite-rhyolite-conglomerate
7	8.6	Very low	29.1	Alluvial terrace-ignimbrite-rhyolite-conglomerate
8	6.6	Very low	48.1	Alluvial terrace, basalt andesite-ignimbrite, rhyolite
9	6.7	Very low	54.1	Alluvial terrace, shale, silt, sandstone
10	16.3	Very low	83.1	Alluvial terrace-silt-limestone

**Table 2:** measured deposition rates of the studied sub-basins in Mighan Watershed

Sub-basins	Sub-basin area (km <sup>2</sup> )	Sediment weight (t/year)	Specific sedimentation (t/km <sup>2</sup> /y)
1	413.6	8755	93.1
2	259.9	5630	194.3

3	352.3	7718	170.4
4	222.7	6021	632.1
5	171	4217	492.8
6	153.3	3224	234.4
7	258.3	5258	95
8	127.3	2615	232.6
9	563.3	11824	43.5
10	118	2509	303.6

In FSM, five factors, namely geology, topography, vegetative cover, gully erosion and basin shape, were utilized to calculate deposition rates. The each item was scored low, medium and high to which 1, 2 and 3 points were assigned, respectively. The numbers were assigned based on field survey and taking advantage of topographical and geological maps (Verstraeten et al, 2003). The scoring method of the factors in FSM has been listed in table (3). The topographical factors of the model have been evaluated based on the mountain sides' slopes and the differential of the lowest and the highest points in the region. The scoring was carried out as follows: one point was given to the low-slope mountain sides (slopes below 4%); two points were given to basins with rolling terrain topography (slopes between 4% and 10%); and, three points were given to basins with high slopes and elevated topography (slopes above 10%) (De Vente et al, 2004; Haregeweyn et al, 2005).

**Table 3:** scoring method of factors in FSM model (Verstraeten et al, 2003)

Row	Factor	Score	Factor explanations
1	topography	1	Mountain sides with very mild slopes and close to the main river with 200-m elevation difference per every 5 kilometers
		2	Mountain sides with mild slopes and close to main river with elevation differentials between 200m and 500m per every 5 kilometers
		3	Steep mountain sides and close to main river with 500-meter elevation differentials per every 5 kilometers
2	Vegetative cover	1	Vegetative cover with good attachment to the soil (vegetative cover accounts for 75% of the basin's surface area)
		2	Vegetative cover with intermediate attachment to the soil (vegetative cover accounts for 25% to 75% of the basin's surface area)
		3	Vegetative cover with loose attachment to the soil (vegetative cover accounts for below 25% of the basin's surface area)
3	Gullies	1	Very low number of gullies or with no gullies
		2	Low number of gullies with visible bottom surfaces
		3	Very large number of gullies with visible bottom surfaces
4	Lithology	1	Limestone, sandstone, conglomerate (low weathering degrees)
		2	Neogene sedimentary facies (gravel and so forth)
		3	Materials with high weathering degrees (loess or marl)
5	Basin shape	1	Fully stretched basins with a main river
		2	Basins with circular and stretched shapes
		3	Circular basins with several main rivers

In FSM, vegetative cover was utilized to explain the soil cover and its resistance to rain erosion. Geological factor is based on the material and composition of the basin's rock units and the various studies have shown that geology plays an important role in the basin's production of sediment. In FSM, gully erosion has been considered as a factor and the scoring was conducted as follows: one point was given to the basins with no gully or basins wherein gullies are rarely found; two points are given to the basins wherein a number of gullies are seen; and, three points are given to the gullied catchments (De Vente et al, 2013). After scoring the fivefold factor, FSM coefficient was obtained as a sum of the factors' coefficients and the basin's erodibility rate was computed using the coefficient as demonstrated in relation (1):

$$SSY = 4139A^{-0.44} + 7.77 \times I_{FSM} - 310.99 \quad \text{Relation (1)}$$

Where, SSY denotes deposition rate in ton per square kilometer; A is the basin's surface area in square kilometer and  $I_{FSM}$  is the model index score.

After the foresaid stage, the score of the fivefold factor of the model was calculated in the intended sub-basins. Then, FSM index was obtained through multiplying the factors' scores (table 4).

**Table 4:** scores of the fivefold factor obtained for the intended sub-basins for calculating FSM index

Sub-basin	Geology	Topography	Basin shape	Vegetative cover	Gully	FSM index
1	1.5	2.4	2	2	1	14.4
2	1.5	0.5	2	3	1	18.9
3	1.8	2	2	3	1	21.6
4	2	2	3	3	2	72
5	2	2	2	3	2	48
6	1.5	2	1	2	2	12
7	1.5	2	1	2	1	6
8	2	1.7	1	2	1	6.8
9	2	1.6	2	2	1	12.8
10	1.5	2.3	2	2	1	13.8

According to the score obtained for the fivefold factor, FSM index score has been given in table 5. Based on the relation (1), the specific deposition rates of the studied basins have also been given in the table. Considering the high differential rates of the estimated and measured values, model coefficients' correction is necessary. After this stage and in order to estimate the specific sedimentation, the relation (1) was used herein again (De Vente et al, 2004 and Haregeweyn et al, 2005).

$$SSY = 4139A^{-0.44} + 7.77 \times I_{FSM} - 310.99 \quad \text{Relation (4)}$$

Where, SSY denotes deposition rate in ton per square kilometer; A is the basin's surface area in square kilometer and  $I_{FSM}$  is the model index score. It is necessary to correct the FSM coefficients because the preliminary coefficients have been developed according to relation (3) for Spain (De Vente and Poesen, 2005) and using them for the other regions of the

world necessitates substitution of other coefficients. Based thereon, the correction or calibration of the model is necessary. Considering the fact that no deposition measurement had been carried out for the studied basins so that FSM calibration could be conducted based on them, empirical FSM calibration plan was used through investigation of the deposition rates of the reservoirs in the small dams in Markazi Province that had been done in 2016 by provincial Agriculture and Natural Resources Research Center. In the aforesaid plan, FSM was calibrated by 11 basins with earth dams (ten years old and with no weirs and mechanical operation in the upper hand side) the observed sedimentation data of which had been obtained through field measurements. It is observed according to figure (1) that the studied watershed basins in the aforementioned plan are in adjacency of Mighan Lagoon and the calibrated FSM in Markazi Province was found applicable to the present study. The corrected FSM equation was transformed as relation (3):

$$SSY = 2589A^{-0.991} + 0.101 \times I_{FSM} - 19.649 \quad \text{Relation (5)}$$

An investigation of the results given in table (5) confirms that the estimated deposition rates using the calibrated FSM are very much close to the measurement results of the basins in such a manner that the deposition rates measured for the studied sub-basins ranges between 43.5 and 632.1 per every square kilometer per year while the estimated deposition rates were found ranging from 20.4 to 27 per square kilometer per year and this is reflective of the high deposition changes in the studied basins.

**Table 5:** deposition rates estimated using FSM for the sub-basins

Sub-basin name	FSM index score	Specific deposition based on the first relation in FSM (t/km <sup>2</sup> /y)	Specific deposition based on the corrected relation in FSM (t/km <sup>2</sup> /y)	Annual deposition mean of the basin (t/y)
1	14.4	93.1	21.2	8755
2	18.9	194.3	21.7	5630
3	21.6	170.4	21.9	7718
4	72	632.1	27	6021
5	48	492.8	24.7	4217
6	12	234.4	21	3224
7	6	95	20.4	5258
8	6.8	232.6	20.5	2615
9	12.8	43.5	21	11824
10	13.8	303.6	21.3	2509

After specific deposition was determined for each of the studied sub-basins, specific erosion was estimated using the sediment delivery ratio (SDR) and the annual deposition and erosion rates of each sub-basin was finally obtained according to surface area (A) values. The following relations were utilized to determine SDR:

$$\text{LogSDR} = 1.8768 - 0.14191 \times \text{Log}10A \quad \text{Relation (8)}$$

$$E = Q_s \div \text{SDR} \quad \text{Relation (9)}$$

In the above relations, A is the basin’s surface area in hectare,  $Q_s$  is the basin’s deposition in ton per hectare and E is the erosion in ton per hectare. In the end, mean annual erosion and deposition rates of each sub-basin was calculated based on surface area and SDR.

**Table 6:** specific and general deposition and erosion rates in the studied sub-basins

Sub-basin name	SDR	Specific erosion (t/km <sup>2</sup> /y)	Total erosion (t/y)
1	0.17	127.1	52551
2	0.18	121.7	31641
3	0.17	128.5	45286
4	0.18	148.7	33102
5	0.19	130.6	22329
6	0.19	109.7	16810
7	0.18	114.3	29522
8	0.20	104.3	13280
9	0.16	131.6	74157
10	0.20	106.9	12605

**Determining the Tectonic Status of the Region Using Quantitative Indices:**

**Valley Width-to-Height (VF) Ratio:**

VF is a geomorphological index that is used to investigate the amount of tectonic activity in a region. Valley width-to-height ratio is usually measured in a specified distance of a mountain front (usually a kilometer from mountain front towards the upper hand section of the river). The index usually demonstrates whether the river engages in scouring its bedding or the erosion substantially takes place laterally towards the river elevated parts and banks. High VF ratios are indicative of low neotectonic outcropping. Therefore, the river erodes the width of its bed and widens it. Low VF values, as well, are suggestive of deep valleys with rivers’ active scouring of their beds accompanied by neotectonic outcropping. The index is calculated as shown below:

$$VF = \frac{2VFW}{(E_{ld} - E_{sc}) + (E_{rd} - E_{sc})} = 2 \times 135 \div (2005.9 - 1952.3) + (2018.9 - 1952.3) = 2.24$$

Where, VF denotes width-to-height ratio of the valley,  $V_{fw}$  is the width of the valley bottom,  $E_{sc}$  is the average valley bottom elevation from the sea level,  $E_{rd}$  is the elevation (from the sea level) of the river’s right hand ridgeline, the line dividing the right side of the river and  $E_{ld}$  is the elevation (from the sea level) of the river’s left hand ridgeline, the line dividing the left side of the river (Ramesht et al, 2012: 39 & 40). To calculate VF ratio in Mighann Watershed, firstly ten different cross-sections were selected (figure 3). Then, average value of all the VF indices obtained was computed and finally the total ratio was obtained for Mighann Watershed (VF=2.24) (table 7). The high values of this ratio are suggestive of low neotectonic outcropping resulting in river’s erosion and widening of its bed.

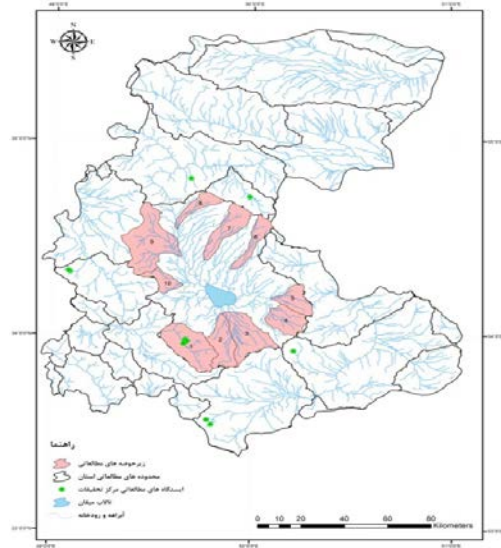


**Figure 3:** the position of the tenfold profile of the VF ratio calculation in Mighann Watershed

**Table 7:** values obtained for VF ratio in Mighann Watershed

Basin number	$V_{fw}$	$E_{sc}$	$E_{rd}$	$E_{ld}$	VF
1	80	2131	2205	2175	1.3
2	100	1825	1895	1888	1.5
3	140	1785	1938	1890	1.08
4	50	1752	1767	1770	3.03
5	400	2096	2190	2150	4.5
6	240	2137	2190	2188	4.61
7	100	1775	1900	1890	0.83
8	100	2027	2044	2044	5.88
9	120	1887	1901	1899	9.23
10	20	2108	2159	2165	0.37
Mean	135	1952.3	2108.9	2005.9	2.24

**Drainage Basin Asymmetry Index (AF):**

Drainage basin asymmetry index relates to the description and understanding of tectonic tilting in zones with larger drainage basin scales. The index signifies the ground tilting as caused by tectonic activities and it is computed as shown below:

$$AF = 100 (A_r/A_t)$$

Where, AF denotes drainage basin asymmetry,  $A_r$  is the surface area of the western part of the basin in respect to the main river stem and  $A_t$  is the total area of the basin. It has to be noted that the western and eastern parts of the basin should be taken into consideration in the same orientation as the river flow. AF values around 50 are suggestive of the existence of asymmetry on both sides of the main water channel hence absence of neotectonic activity; in case that the watershed is found influenced by tectonic forces, the AF value obtained might be below or above 50. AF values above 50 are indicative of rising on the west side of the main water channel and AF values below 50 are reflective of rising on the east side of the main water channel (Ramesht et al, 2012: 38 & 39). According to the value obtained herein for AF, 47.6, (table 8), and considering the fact that Mighann Watershed has undergone tilting towards the eastern side of the drainage basin and

knowing that the rivers on the left side (western mane) are longer than the opposite side, it can be figured out that the tectonic activities in this watershed are very intensive a sign of which can be traced in the ground tilting towards the right side (eastern part) and side processes (like landslide and landfall).

**Table 8:** AF values obtained for Mighan Watershed

Sub-basin's number	A <sub>r</sub>	A <sub>t</sub>	AF
1	116.37	258.25	45.06
2	54.98	117.95	46.61
3	210.3	413.55	50.85
4	305.4	563.31	54.21
5	70.49	127.26	55.39
6	136.68	222.65	61.38
7	66.75	171.02	39.03
8	115.44	352.29	32.76
9	92.36	259.91	35.53
10	73.69	153.25	48.08
Mean	124.2	263.9	47.06

**River's Longitudinal Gradient Index (SL):**

The index pertains to the power of current. The available river force within a separate and specified cross-section is an important hydrological variable because it is connected with the ability of the river in eroding its bed as well as carrying erosional materials. The index is obtained as shown in the following relation:

$$SL = \frac{\Delta H}{\Delta L} \times L$$

Where, ΔH is the differential of the two specified points, ΔL is the horizontal distance between the same two points and L is the river length from the central point to the river head. It can be stated based on the above relation that  $\frac{\Delta H}{\Delta L}$  is in fact the very relation that can be used for basin's slope. The river power depends on its discharge rate and bed slope. This way, it can be comprehended that the index is sensitive to slope changes and this same issue enables the evaluation of the relationships between tectonic activities, rock strength and topography. High SL values in rocks featuring low strength or in rocks with identical strength rates can be indicative of active and young neotectonic activities (Ramesht et al, 2012: 45 & 46). The longitudinal gradient index values for Mighan Watershed were determined using digital model of elevation and organization of the geographical information. To calculate SL index in Mighan Watershed, the river's longitudinal profile was first drawn. Then, SL value was measured for the entire Mighan Watershed path from the outlet to the source considering the mountainous nature of the region and according to the various elevations of the sub-basins in the specified elevation intervals. Mean value of all the obtained SL indices was computed and, in the end, total SL value was obtained for the entire Mighan Watershed equal to 353.4 (table 9) which is suggestive of the region's activeness in terms of neotectonic movements and outcropping.

**Table 9:** SL values obtained for Mighan Watershed

Sub-basin number	H	L	L	SL
1	792	33559.6	18729.5	442.1
2	345	15486.6	10574.2	235.5
3	611	25933.9	16454.7	387.6
4	228	25461.2	17961.1	16.08

5	557	24068.1	14366.1	332.4
6	751	19937.4	11572.3	435.9
7	164	17179.6	10281.6	92.7
8	940	30510.2	16914.9	521.1
9	770	30043.9	19346.5	495.8
10	661	30698.3	18022.8	388.1
Mean	581.9	25388.8	15422.3	353.4

**Transverse Topography Symmetry Factor (T Index):**

The index can determine the symmetry hence activeness or inactiveness of the region. The index is computed using the following relation:

$$T = \frac{D_a}{D_d}$$

Where, T is the transverse topography symmetry, D<sub>a</sub> is the distance of the active meandering belt from the midline of the drainage basin, D<sub>d</sub> is the distance of the drainage basin's to its borderline. T-index is zero in completely symmetrical basins but the index increases with the decrease in the basin's symmetry and approaches unity. It is assumed that the slope of the strata does not have much of an effect on the migration of the river's main channel in which case the general and overall migration becomes the factor contributing to the ground tilt towards a special orientation. Thus, T index is reflective of a vector with specific direction and [1, 0] values. The analysis is more appropriate for drainage basins with dendritic patterns. Higher T index ranges are permissible in regions where the evaluation of valley branch is as good as the evaluation of the primary valley or body (Ramesht et al, 2012: 42 & 43). To calculate T index in Mighan Watershed, D<sub>a</sub> and D<sub>d</sub> values were measured in 10 sub-basins from the outlet to the headwater. Then, mean value of all the measurements was computed in order for the obtained value to be expressive of the entire basin path. The amount of T index for Mighan Watershed was found equal to 0.24 (table 10). It can be figured out based on the T index values obtained for Mighan Watershed that the basin is in an active state of neotectonics. Besides confirming the T-index value, the geomorphological evidences extant for Mighan Watershed can be used to find out such cases as drainage network's asymmetry and the majority of the water channel's lengthiness on the left hand side of Mighan Watershed.

**Table 10:** T index values in Mighan Watershed

Sub-basin number	T
1	0.17
2	0.14
3	0.16
4	0.15
5	0.39
6	0.15
7	0.41
8	0.26
9	0.21
10	0.41
Mean	0.24

**Basin Shape (BS) Index:**

Drainage basin shape index is an indicator used in tectonic activity assessments. Usually, the basins with active tectonic are oblong in shape. According to the activity cessation or

erosional processes' prevalence, the basin's shape gradually becomes circular in the course of time and BS index is decreased. The index is obtained from the following relation:

$$BS = B_i / B_w$$

Where,  $B_i$  is the length of the watershed encompassing the extent from the basin's outlet to the outermost part of the basin and  $B_w$  is the width of the watershed. High BS values are indicative of active neotectonics in a watershed (Ramesht, 2012: 41 & 42) whereas lower BS values are more reflective of circular basins situated in regions with low tectonic activities (inactive) (Ramirez-Harira, 1998). Based on El-Hamduni's categorization, BS index values for basins are as explained below:

- BS>4 → Active Basin (Class 1)
- BS>3-4 → Semi-Active Basin (Class 2)
- BS>4 → Inactive Basin (Class 3)

BS index was obtained equal to 3.5 for Mighann Watershed (table 11) and it signifies that Mighann Watershed is positioned in a semi-active tectonic zone.

**Table 11:** values pertaining to BS index in Mighann Watershed

Sub-basin number	$B_w$	$B_i$	BS
1	7583.16	34683.4	4.5
2	10987.42	20224.7	1.8
3	14762.29	32054.8	2.1
4	25691.99	35325.4	1.3
5	4873.6	25401	5.2
6	13206.1	2038.2	1.5
7	12492.37	21503.5	1.7
8	12802.66	32294.4	2.5
9	10517.29	30837.9	2.9
10	2675.38	32622.7	11.7
Mean	11569.2	28528.6	3.5

**River Meander Scrolls (S):**

High meandering rates are indicative of the relative stability of the neotectonic activity of the basin. The index is computed as shown in the relation below:

$$S = c/v$$

Where, C is the river length and V is the valley length on a direct line. Higher S values signify that the river is in equilibrium and the lower S values are suggestive of active neotectonics in a basin (Ramesht et al, 2012: 45). The S value obtained for Mighann watershed is equal to 1.21 (table 12). Therefore, according to the index value, it can be concluded that the studied region has not yet reached equilibrium in terms of tectonic activity and the internal and tectonic forces are still playing a considerable role in the evolution of the region.

**Table 12:** S values obtained for Mighann Watershed

Sub-basin number	C	V	S
1	37.4	33.5	1.11
2	21.1	15.4	1.37
3	32.9	26.1	1.26
4	35.9	25.4	1.41
5	28.7	24.5	1.17
6	23.1	20	1.15
7	20.5	18.1	1.13
8	33.8	30.3	1.11
9	38.6	30	1.28
10	36	30.6	1.17
Mean	30.8	25.3	1.21

Extracting the Statistical Relationships of the erosion and deposition values for the sub-basins in Mighann Watershed using geomorphological indices:

**4. Statistical Test Results:**

**Data Normality Results:**

In this stage of the data analysis, it is necessary to investigate the data distribution normality. As shown in the following table, the skewness and kurtosis values are in a range from +2 to -2 indicating the data distribution normality.

**Table 13:** values pertaining to normality of the geomorphological indices and erosion and deposition rates

Index	Erosion	Sediment	AF	VF	BS	T	S	SL
Skewness	0.425	1.846	-0.122	0.967	1.300	0.740	0.850	-0.720
Kurtosis	-0.114	1.808	-0.765	0.232	1.726	-1.168	-0.655	-0.593

**Correlation Test Results:**

**Geomorphological Indices Correlation with Erosion and Deposition Values:**

Figures (4-9) illustrate the correlation between the geomorphological indices and erosion and deposition values. Table (14), as well, gives the  $R^2$  (determination coefficients) and P-values (significance level). According to the results, it becomes clear that the highest correlation between the geomorphological indices and erosion pertains to BS index and it is only this index that is significantly correlated with erosion in a 95% confidence level. Moreover, the highest correlation of the geomorphological indices with deposition was found belonging to BS and it is only BS that is significantly correlated with deposition in a 95% confidence level.

**Table 14:** statistical results of correlation between geomorphological indices and erosion and deposition values

Geomorphological index	Erosion		Deposition	
	$R^2$	P-value	$R^2$	P-value
AF	0.31	0.09	0.03	0.62
VF	0.13	0.31	0.14	0.29
BS	0.40	0.05	0.78	0.00
T	0.32	0.16	0.12	0.33
S	0.06	0.49	0.13	0.30
SL	0.00	0.93	0.11	0.36

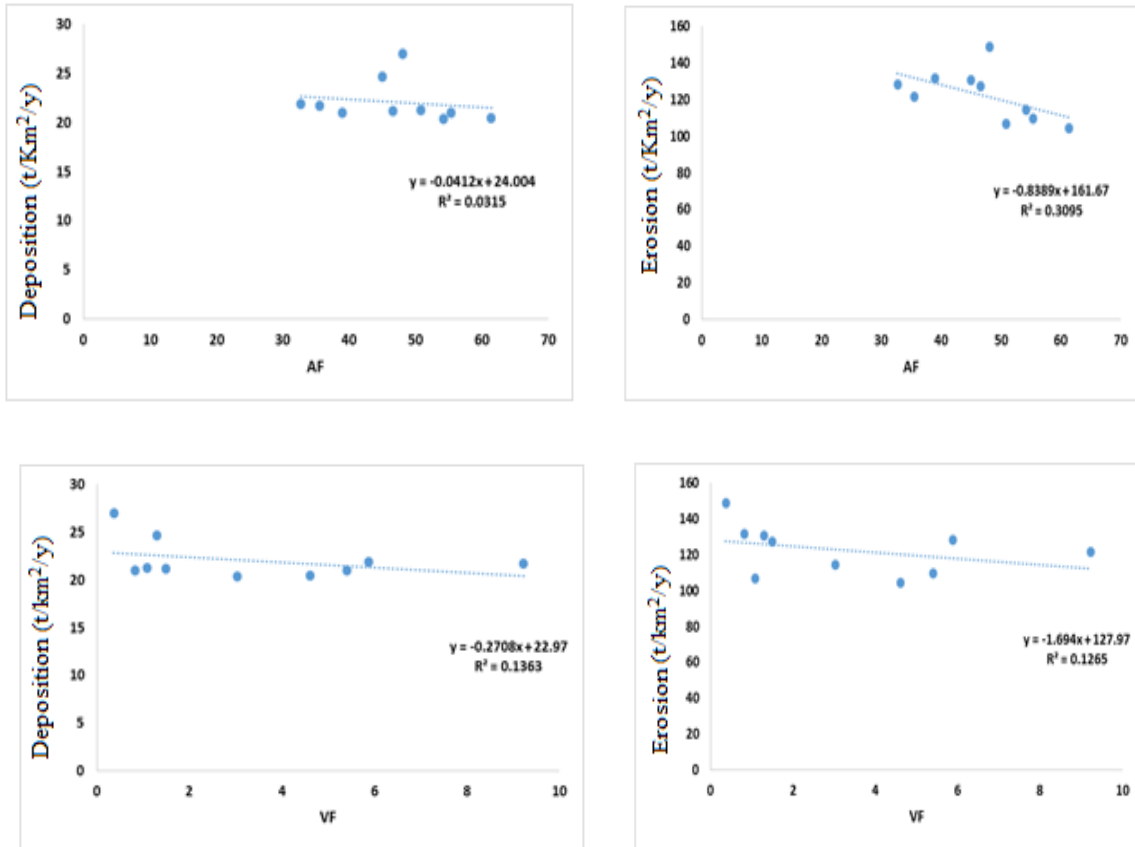


Figure 5: correlation between VF and erosion and deposition rates

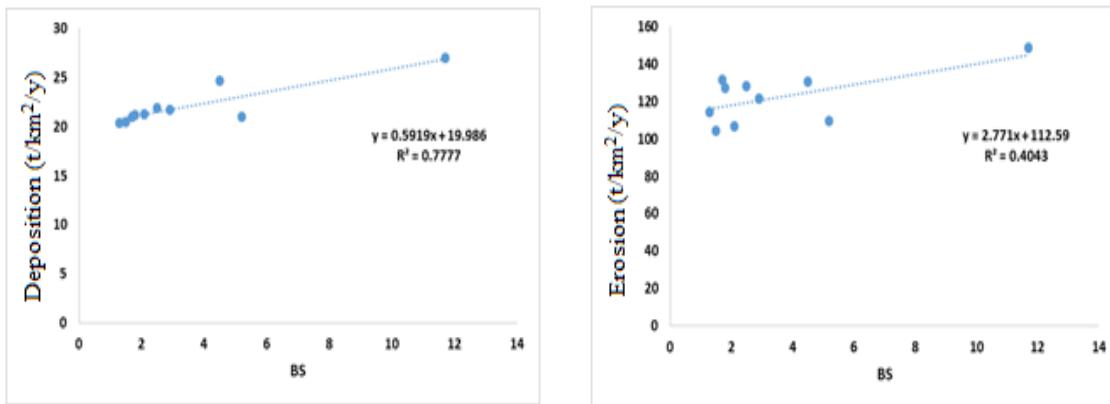


Figure 6: correlation between BS and erosion and deposition values



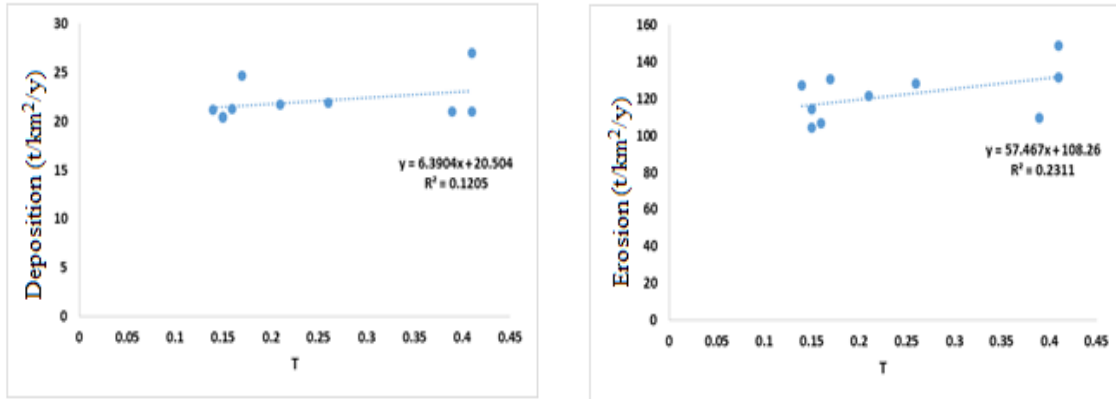


Figure 7: correlation between T index and erosion and deposition values

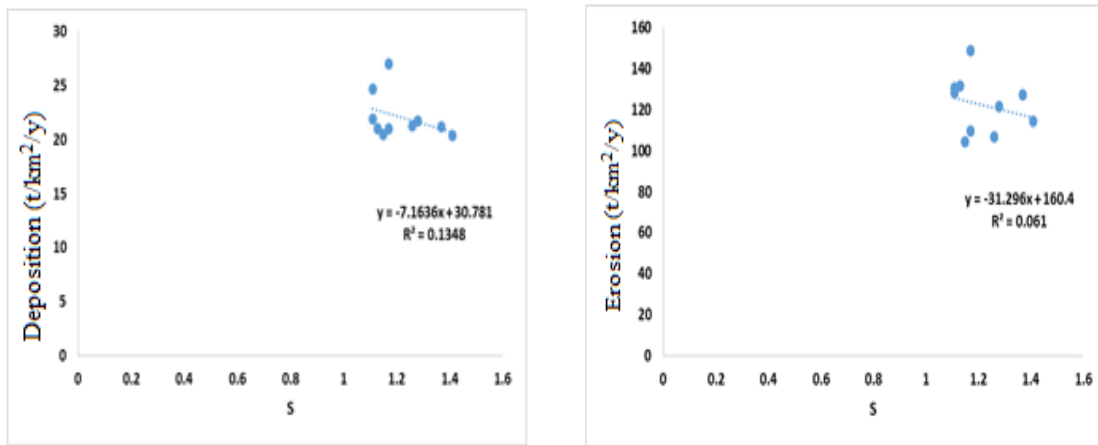


Figure 8: correlation between S index and erosion and deposition values

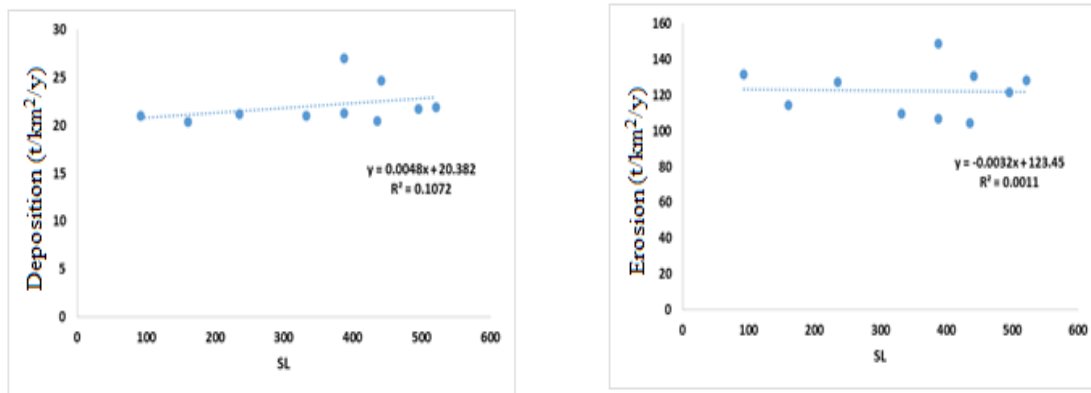


Figure 9: correlation between SL index and erosion and deposition values

**Results of Multivariate Regression Test:**

In this stage, the corresponding equation is constructed according to the significant relationship between the various indices and erosion and deposition values.

**Equation between Geomorphological Indices and Erosion and Deposition Values:**

Table (15) shows that R<sup>2</sup> value for illustrating the equation between the geomorphological indices and erosion is 0.951 which is indicative of a strong relationship. Also, P-value is below 0.05 which confirms the significance of the relationship.

But, according to table (16), amongst the parameters, only AF and BS are significant. Thus, the equation between the geomorphological indices and erosion takes the following form:

$$\text{EROSION} = -1.231\text{AF} + 5.610\text{BS} + 293.769$$

**Table 15:** multivariate regression correlation of the geomorphological indices and erosion

Model	R	R <sup>2</sup>	Degree of freedom	Significance level
1	0.975 <sup>a</sup>	0.951	9	0.045

**Table 16:** multivariate regression coefficients of geomorphological indices and erosion

Model	Coefficients		T	Significance	
	B	Standard error			
1	(constant)	293.769	66.859	4.394	0.022
	AF	-1.231	0.227	-5.433	0.012
	VF	0.773	1.321	0.585	0.600
	BS	5.610	1.525	3.679	0.035
	T	-104.806	50.636	-2.070	0.130
	S	-64.371	37.986	-1.695	0.189
	SL	-0.092	0.041	-2.246	0.110

Table (17) shows that R<sup>2</sup> value for illustrating the equation between geomorphological indices and deposition is 0.996 which is reflective of a strong relationship. Also, the total P-value is found below 0.05 confirming the significance of the relationship. But, according to table (18), amongst the parameters all, except VF, are significant. Thus, the equation between the geomorphological indices and erosion takes the following form. In this relation, AF, T, S and SL are negatively correlated with deposition and BS is positively associated with deposition.

$$\text{SEDIMENT} = -0.087\text{AF} + 0.902\text{BS} - 15.475\text{T} - 8.997\text{S} - 0.006\text{SL} + 39.869$$

**Table 17:** multivariate regression correlation between geomorphological indices and deposition

Model	R	R <sup>2</sup>	Degree of freedom	Significance level
1	0.998 <sup>a</sup>	0.996	9	0.01

**Table 18:** multivariate regression coefficients of geomorphological indices and deposition

Model	Coefficients		T	Significance	
	B	Standard error			
1	(constant)	39.869	3.109	12.822	0.001
	AF	-0.087	0.011	-8.290	0.004
	VF	-0.003	0.061	-0.044	0.968
	BS	0.902	0.071	12.725	0.001
	T	-15.475	2.355	-6.571	0.007
	S	-8.997	1.767	-5.093	0.015
	SL	-0.006	0.002	-3.220	0.049

**5. Conclusion:**

Corresponding to the normal method of work, FSM was calibrated based on the report issued in FSM empirical model calibration research plan through investigating the sediment in the small dams in Markazi Province and it was used to estimate deposition rates in 10 studied sub-basins in Mighan Watershed. According to the results, the lowest erosion and deposition rates in sub-basin 6 were 104.3t/km<sup>2</sup>/y and

20.5t/km<sup>2</sup>/y and the highest erosion and deposition rates in sub-basin 10 were 148.7t/km<sup>2</sup>/y and 27t/km<sup>2</sup>/y, respectively. Based on the results, the increase in BS, as a morphological index, causes an increase in the erosion and deposition rates but AF, T, S and SL were found negatively associated with deposition. Amongst the geomorphological indices, SL was found playing a more effective role in the creation of erosion differences between the sub-basins. Since BS is directly correlated with erosion and deposition in the studied sub-basins and the studied region is considered young in terms of tectonic activity, the erosion processes are very variable. The same result was also proved in the current research paper and it was demonstrated that the young basins undergo more intensive erosion. BS, an index indicating the basin shape, is higher in value in more oblong basins and it can be concluded that the region is undergoing a high tectonic activity and erosion since the majority of the studied basins were oblong in shape. In sum, the results obtained in the present study indicated that the erosion and sedimentation potentials in Mighan Watershed's sub-basins are variable and an array of geomorphological indices is effective thereon. According to the results correlation between the geomorphological indices and erosion and deposition values, it was concluded that the increase in BS (basin shape index) brings about an increase in the erosion and deposition rates. The results of multivariate regression, as well, demonstrated that unlike AF (drainage basin asymmetry index) that is inversely correlated with erosion, there is a positive and direct relationship between BS and erosion. BS index was also found having a positive relationship with deposition. Corresponding to the results, it can be stated that there is an inverse relationship between such indices as AF, T (transverse topographical symmetry index), S (river meander scroll index) and SL (river's longitudinal gradient index) with deposition.

**REFERENCES**

- Atapourfard, A., Moradi Sharaf, M. and Shoaee, G. (2012) The application of FSM model for the prediction of sediment yield in Tehran basin, Nature and Science, 10(9): 105-112.
- Azor, A., Keller, E.A., Yeats, R.S., (2002), "Geomorphic indicators of active fold growth: South Mountain-Oak Ridge Ventura basin, southern California", Geological Society of America Bulletin 114, 745-753.
- Bull, W.B., McFadden, L.D., (1977), "Tectonic geomorphology north and south of the Garlock fault, California. In: Doehring, D.O. (Ed.)", Geomorphology in Arid Regions. Proceedings of the Eighth Annual Geomorphology Symposium. State University of New York, Binghamton, pp. 115-138.
- De Vente, J., J. Poesen & G. Verstraeten. )2005(. The application of semi-quantative methods and reservoir sedimentation rates for the prediction of sediment yield in Spain. Journal of Hydrology. 305: 63-86.
- De Vente, J., J. Poesen and G. Verstraeten. )2004(. The application of semi-quantitative methods and reservoir sedimentation rates for the prediction of

- basin sediment yield in Spain. *Journal of Hydrology*, 305: 63–86.
6. De Vente, J., J. Poesen. )2005(. Predicting soil erosion and sediment yield at the basin scale: Scale issues and semi-quantitative models. *Earth-Science Reviews* 71: 95–125.
  7. De Vente, J., J. Poesen, P. Bazzoffi, A. Van Rompaey and G. Verstraeten. )2006(. Predicting catchment sediment yield in Mediterranean environments: the importance of sediment sources and connectivity in Italian drainage basins. *Earth Surface Processes and Landforms*, 31: 1017-1034.
  8. De Vente, J., Poesen, J., Verstraeten, G., Govers, G., Vanmaerck, M., Van Rompaey, A., Arabkhedrie, M., and Boix-Fayos, C.) 2013(. Predicting soil erosion and sediment yield at regional scales: Where do we stand *Earth-Science Reviews*, 127: 16-29.
  9. Douglas W. Burbank, Robert S. Anderson (2001), "Tectonic Geomorphology", Blackwell Science, Lt.
  10. EL Hamdouni, R.E., Irigaray, C., Fernandez, T., Chacon, J., Keller E.A., (2008), "Assessment of Relative Active Tectonic, South West Border of the Sierra Nevada (Southern Spain)", *Geomorphology*, 96, 150-173.
  11. Goldman, S., K. Jakson, P. Ebursztynsky, (1986), *Erosion and sediment handbook*, p. 1-47.
  12. Haregeweyn, N., J. Poesen, J. Nyssen, G. Verstraeten, J. D. Vente, G. Govers, S. Deckers and J. Moeyersons.) 2005(. Specific sediment yield in Tigray-Northern Ethiopia: Assessment and semi-quantitative modeling. *Geomorphology*. 69. pp: 315-331.
  13. Kaviyan, Ata'ollah; Asgariyan, Raziye; Nateghi, Taravash; Ja'afariyan Jelodar, Zainab and Safary, Ata, (2014), "evaluation of the efficiency of EPM, PSIAC and FSM models in the estimation of sediment yield in rangelands (case study: Sorkh Abad Watershed in Mazandaran Province)", *seasonal scientific-research journal of Ahar's geographical space*, 14(48): 57-79
  14. Keller, E.A., Pinter, N., (1996), "Active, Tectonics: Earthquake, Uplift and Landscape, Prentice Hall Publication", London.
  15. Keller, E.A., Pinter, N., (2002), "Active Tectonics: Earthquakes, Uplift, and Landscape. Prentice Hall", New Jersey.
  16. Madadi, Aghil; Reza'ei Moghaddam, Muhammad and Hussein Raja'ei, Abdulhamid. (2004), "analyzing the neotectonic activities using geomorphological methods in northwestern slopes of Talesh (Baghroudagh)", *geographical studies*, (48): 123-138
  17. Mirzakhany, Bahareh, (2011), "geomorphological changes in Mighan Watershed during Quaternary Era", MA dissertation, Teacher Training University, Tehran Branch
  18. Mohammadiha, S., H.R. Peyrowan, R. Mousavi Harami, S. Feiznia. )2011(. Evaluation of soil erosion and sediment yield using semi quantitative models: FSM and MPSIAC in Eivaneke watershed and the sub-basins (Southeast of Tehran/Iran). *Journal of American Science*, 7(7): 234-239.
  19. Mohammadiha, Shirin; Pirovan, Hamid Reza; Mousavi Harami, Reza; Faizniya, Sadat and Bayat, Reza, (2011), "investigation of the erosion rate and sediment yield in Eywanaki Watershed using FSM and MPSIAC and sediment-measurement station", *stratigraphic and sedimentological studies*, 45(27): 31-48
  20. Molin, P., Pazzaglia, F.J., Dramis, F., (2004), "Geomorphic expression of active tectonics in a rapidly deforming forearc, sila massif, Calabria, southern Italy", *American Journal of Science* 304, 559–589.
  21. Nabipay Lashkariyan, Sa'eid; Hashemi, Sayyed Ali Asghar and Shadfar, Samad, (2013), "investigating the efficiency of FSM in estimating total sediment yield of Semnan Province", v.5, *scientific and research journal of watershed management and engineering*, (1): 51-58
  22. Ramesht, Muhammad Hussein; Ara'a, Hayedeh; Shayan, Siyavash and Yamani, Mojtaba, (2012), "evaluation of the accuracy and authenticity of the geomorphological indices using geodynamic data (case study: Jajrud Watershed in northeast Tehran", *journal of geography and environmental planning*, (2): 35-52
  23. Ramirez- Herrera, M.T., (1998) "Geomorphic Assessment of active tectonic in the Acambay Graben", *Mexican Volcanic belt Earth Surface and landforms* 23,317-322.
  24. Rockwell, T.K. et al. 1984. Alate Pleistocene-Holocene Soil Chronosquence in the Ventura Basin Southern California U.S. Aallen and Unwin, London. 309-327.
  25. Saffary, Amir and Mansoury, Reza, (2013), "relative evaluation of the tectonic activities in the upper part of Kangir Watershed in Eywan-e-Gharb using geomorphological indices", *journal of geography and urban logistics*, (7): 35-50
  26. Silva, P.G., Goy, J.L., Zazo, C., Bardajm, T., (2003), "Fault generated mountain fronts in Southeast Spain: geomorphologic assessment of tectonic and earthquake activity", *Geomorphology* 250, 203–226.
  27. Solaimani, Shahriyar, (1999), "guidelines on the identification of active and young tectonic movements with a look at old seismological background", 1st ed., *international seismology and earthquake engineering institution*
  28. Verstraeten, G., J. Poesen, J. de Vente & X. Koninckx. )2003(. Sediment yield variability in Spain: A quantitative and semiquantitative analysis using reservoir sedimentation rates. *Geomorphology*. 50 (4) 327–348.
  29. Wells, S.G., Bullard, T.F., Menges, C.M., Drake, P.G., Karas, P.A., Kelson, K.I., Ritter, J.B., and Wesling, J.R. )1988(. Regional Variations in Tectonic Geomorphology along a Segmented Convergent Plate Boundary. *Pacific Coast of Costa Rica. Geomorphology*, 1, 239–265.
  30. Zulfaghary, Morteza; Hashemi, Muhammad Naser and Haidary, Maryam, (2010), "investigating the

spatial displacements of rainfall and precipitation volume in Mighan Watershed”, collection of articles from the second conference on Iran’s central lagoons, Islamic Azad University, Amir Kabir, Arak